

Interactions of Cobalt Carbonyls with Oxide Surfaces. 3. Dicobalt Octacarbonyl and Tetracobalt Dodecacarbonyl in Zeolites

ROGER L. SCHNEIDER, RUSSELL F. HOWE,[†] and KENNETH L. WATTERS*

Received October 17, 1983

Reactions of $\text{Co}_2(\text{CO})_8$ and $\text{Co}_4(\text{CO})_{12}$ with A, X, and Y zeolites have been studied with IR spectra and quantitative and qualitative measurements of gas-phase species generated in the reactions. The carbonyls were added to the zeolites by direct sublimation at room temperature. Reactions with the Na-A zeolite are limited by the inability of the carbonyls to pass through the apertures to the cavities of this zeolite. Dicobalt octacarbonyl penetrates the faujasite (X and Y zeolite) framework, where it is converted quickly, in vacuo, to $\text{Co}_4(\text{CO})_{12}$, $[\text{Co}(\text{CO})_4]^-$, and other unidentified cobalt carbonyl species with $\nu(\text{CO})$ bands between 1900 and 2030 cm^{-1} . Once formed in this manner, the tetracobalt cluster compound is too large to exit the zeolite but is converted, by mild heating, to the tetracobalt anion and the novel cobalt carbonyl species. Heating above 425 K results in irreversible decarbonylation in all the zeolite-supported cobalt carbonyls. Under certain conditions and when the support is NaX, the $\nu(\text{CO})$ spectrum is dominated by bands assigned to $[\text{Co}(\text{CO})_4]^-$, while all other cobalt carbonyls are present in relatively small amounts. Manometric studies, which were used to determine the ratio of CO/Co on such samples, suggest disproportionation of the parent carbonyl to Co(II) and $[\text{Co}(\text{CO})_4]^-$ occurs. All species on the zeolite surfaces, except $\text{Co}_4(\text{CO})_{12}$, are quickly oxidized by O_2 . This permits the preparation of samples in which the only cobalt carbonyl species remaining is $\text{Co}_4(\text{CO})_{12}$. Oxidation by $^{18}\text{O}^{18}\text{O}$ evolves CO, which contains a large fraction of C^{18}O . Mechanisms involving reversible formation of hydroxy carbonyl or peroxy carbonyl ligands are invoked to explain this exchange of oxygen atoms from molecular oxygen into the CO. Shifts in $\nu(\text{OH})$ bands of an H-Y zeolite and $\nu(\text{CO})$ bands of bridging carbonyls provide evidence for hydrogen bonding between hydroxyl hydrogens and bridging carbonyl oxygens on this support. On the basis of symmetry considerations and internuclear distances, a C_{3v} bonding site is proposed at the supercage windows. The room-temperature reactions observed for the cobalt carbonyls on the zeolites and on other refractory oxides are discussed in terms of the known solution chemistry of these carbonyl complexes and the observed interactions between the carbonyls and the oxide surfaces.

Introduction

Another paper¹ reports results of an investigation of $\text{Co}_2(\text{CO})_8$ and $\text{Co}_4(\text{CO})_{12}$ deposited on silicas, γ -alumina, and a silica-alumina surface. A cardinal observation was the rapid and nearly stoichiometric conversion, in vacuo, of $\text{Co}_2(\text{CO})_8$ to $\text{Co}_4(\text{CO})_{12}$ on the silicas and silica-alumina. On γ -alumina, evacuation of supported $\text{Co}_2(\text{CO})_8$ generated other species and only small quantities of supported $\text{Co}_4(\text{CO})_{12}$. The new species formed on $\gamma\text{-Al}_2\text{O}_3$ presumably are sub-carbonyl complexes of cobalt; these may be reversibly carbonylated to regenerate the parent complexes, $\text{Co}_2(\text{CO})_8$ and $\text{Co}_4(\text{CO})_{12}$, on the alumina. Facile isotopic exchange reactions also were observed for most of the supported cobalt carbonyls, and oxidation by isotopically labeled O_2 produced not only C^{18}O_2 but also C^{18}O .

Zeolites may be considered, in some respects, to have chemical properties intermediate between those displayed by silicas, on one hand, and aluminas on the other. Moreover, the uniformity of adsorption sites within a crystalline zeolite affords better opportunity for determining, from spectroscopic and other data, the details of the adsorbent/adsorbate interaction. Finally, the size selective properties of a zeolite would preclude entry or exit by cluster compounds larger than the windows in the zeolite framework; indeed, $\text{Co}_4(\text{CO})_{12}$ should be too large to pass through these apertures for many zeolites. Zeolite cage size also would prevent formation of large metal atom aggregates within the zeolite framework and might, therefore, provide steric stabilization of small clusters.

The study of the cobalt carbonyls $\text{Co}_2(\text{CO})_8$ and $\text{Co}_4(\text{CO})_{12}$ on oxide supports has been extended to include zeolites as supports for the reasons cited above and because of the important and unique properties of zeolites as catalyst supports and materials. The cobalt carbonyls have been investigated by IR spectroscopy and by gas analysis techniques as they are deposited by sublimation onto the dehydrated framework zeolites, Na-X, Na-Y, Na-A, H-Y, and D-Y.

Experimental Section

The cobalt carbonyl compounds, solvents, and gases employed in this study were obtained, purified, and used as described in the preceding paper; the gas handling system and spectroscopic equipment also have been described previously.¹⁻³ The Na-Y zeolite ($a_s = 880 \text{ m}^2/\text{g}$, monolayer equivalent) was Linde SK-40, Na-A was Linde 4A MS-409, and Na-X ($a_s = 870 \text{ m}^2/\text{g}$, monolayer equivalent) was Linde 13X. All zeolites were washed in doubly distilled water and then calcined in air at 675 K prior to use. Some were first washed in boiling distilled water to more effectively remove silicate impurities. This extra treatment had no effect upon the results. Following calcination, the zeolites were formed, at 8000 psi (55 MPa), into wafers of thickness 5–10 mg/cm^2 ($\approx 0.3 \text{ mm}$) for IR spectra and gas manometry. High-temperature treatments (500–800 K) were attained by very gradually heating, under vacuum, to the desired temperature so as to avoid loss of crystallinity through self-steaming. Samples treated in this manner show no evidence, by X-ray powder pattern, of loss of crystallinity. The zeolite supports were treated, in vacuo, at temperatures ranging from 500 to 800 K immediately preceding sublimation of the cobalt carbonyl onto the support. The pretreatment temperature used for a given sample is included with the description of that experiment.

The H-Y zeolite samples were prepared by ion exchange of the Linde SK-40 Na-Y zeolite with a 0.1 F solution of NH_4NO_3 , following literature procedures.⁴ The extent of exchange of NH_4^+ for Na^+ , determined by flame photolysis analysis for sodium in the filtrate and washings, was 91%. Wafers of the then zeolite were converted to H-Y zeolite in the IR cell by heating at 675 K, in vacuo. This also effected dehydration of the zeolite. The D-Y zeolite was prepared by the gas-phase exchange of H-Y with D_2 at 675 K.

Solution impregnation was achieved in a cell fitted with a special Schlenk vessel, as shown in Figure 1. The adsorbate, $\text{Co}_2(\text{CO})_8$, was

- (1) Schneider, R. L.; Howe, R. F.; Watters, K. L. *Inorg. Chem.*, preceding paper in this issue.
- (2) Schneider, R. L.; Howe, R. F.; Watters, K. L. *J. Catal.* **1983**, *79*, 298.
- (3) Watters, K. L. *SIA Surf. Interface Anal.* **1981**, *3*, 55. Schneider, R. L. Ph.D. Dissertation, University of Wisconsin—Milwaukee, 1982.
- (4) Kerr, G. T. "Molecular Sieves", Meier, W. M., Uytterhoeven, J. B., Eds.; American Chemical Society: Washington, DC, 1973; Adv. Chem. Ser. No. 121, pp 219–229.
- (5) Watters, K. L.; Howe, R. F.; Chojnacki, T. P.; Fu, C. M.; Schneider, R. L.; Wong, N. B. *J. Catal.* **1980**, *66*, 424.

[†] Present address: Department of Chemistry, University of Auckland, Auckland, New Zealand.

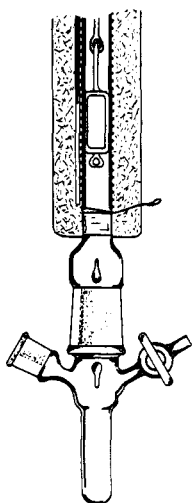


Figure 1. Diagram of the special adaptation of the cell used for loading cobalt carbonyls onto oxide supports by solution impregnation. The 14/20 F-joint pictured is fitted with a rubber septum through which the carbonyl solution is injected into or withdrawn from the well. Complete cell diagrams are shown in ref 1 and 3.

Table I. Assignment of $\nu(\text{CO})$ Bands

sample (species)	obsd freq ^a
<i>Co₂(CO)₈/Na-Y</i>	
<i>Co₂(CO)₈</i>	2127, 2060, 2024, 1820, 1794
<i>Co₄(CO)₁₂</i>	2121, 2078, 2053, 1851, 1812
<i>Co(CO)₄⁻</i>	1938, 1901, 1868
sub-carbonyls ^b	2022, 1965, 1946
<i>Co₂(CO)₈/Na-X</i>	
<i>Co₂(CO)₈</i>	2128, 2064, 2034, 1806
<i>Co₄(CO)₁₂</i>	2108, 2080, 1819
<i>Co(CO)₄⁻</i>	1941, 1891, 1870
sub-carbonyls ^b	2036, 1966, 1941

^a Frequencies given in cm^{-1} . ^b One or more species that appear to be in equilibrium with each other and/or with $\text{Co}_4(\text{CO})_{12}$.

dissolved in dry deoxygenated *n*-pentane that was distilled into the Schlenk flask attachment containing the $\text{Co}_2(\text{CO})_8$. The IR wafer then was lowered several times into the solution and the extent of loading monitored by observing the intensity of $\nu(\text{CO})$ bands that developed on the support.

Sublimation loading was accomplished as described in the preceding paper and yielded loadings of 1–3% cobalt by weight.

Results

IR Spectra. On Na-Y Zeolites. In the study of $\text{Co}_2(\text{CO})_8$ sublimed onto silica,¹ a CO-inhibited conversion to $\text{Co}_4(\text{CO})_{12}$ /silica was observed, the conversion being completely inhibited at $P > 20$ torr. Sublimation of $\text{Co}_2(\text{CO})_8$ onto Na-Y zeolite under CO produces a yellow sample that changes to brown upon removal of CO from the cell. To better understand the chemistry of $\text{Co}_2(\text{CO})_8$ on the zeolites, experiments were conducted in which $\text{Co}_2(\text{CO})_8$ was sublimed under CO onto the support and IR spectra obtained for the sample under CO. Figure 2 presents the IR spectral results in the 1700–2150- cm^{-1} $\nu(\text{CO})$ region for such an experiment. The bands at 2127, 2060, 2024, 1820 (sh), and 1794, in composite A, are assigned to $\text{Co}_2(\text{CO})_8$ adsorbed on the zeolite (Table I). This particular set of bands is not observed when sublimation is conducted under a vacuum; instead, a set of bands identical with those in spectrum m, composite D, of Figure 2 (2Dm) develops. Indeed, the gradual removal of CO from the cell, after preparation of the sample responsible for spectrum 2Ag, induces the progressive conversion to the species responsible for spectrum 2Dm. The bands at 2121, 2078, 2053, 1851, and 1812 cm^{-1} in spectrum 2Dm are assigned to supported Co_4 -

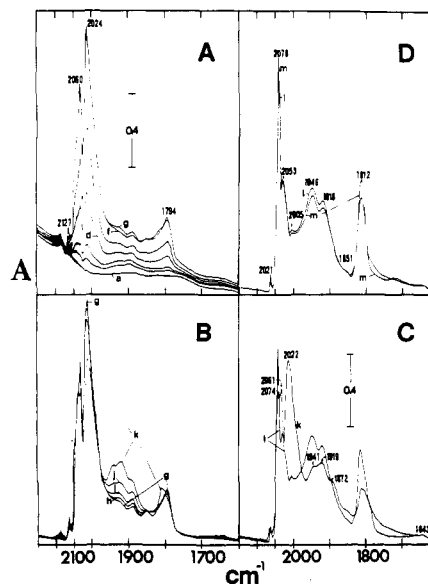


Figure 2. IR absorbance spectra in the carbonyl region for $\text{Co}_2(\text{CO})_8$ sublimed onto Na-Y that had been pretreated, in vacuo, at 675 K for 8 h. Composites B–D are difference spectra with Na-Y bands subtracted. Composite A shows spectra that develop as the zeolite is loaded under 60 torr of CO, with $\text{Co}_2(\text{CO})_8$. The tube containing solid cobalt carbonyl was open continuously to the sample. Individual spectra a–g with loading times (min) are as follows: (a) 0, background; (b) 16; (c) 32; (d) 79; (e) 139; (f) 226, sublimator closed at 232; (g) 296. Spectra h–m show results of reducing CO pressure in the cell subsequent to loading. The pressure (torr) and the total time (min) the system was at the pressure before recording a spectrum are as follows: (h) 45, 67; (i) 29, 46; (j) 14, 48; (k) 5.9, 51; (l) 10^{-2} , 25; (m) 10^{-2} , 400.

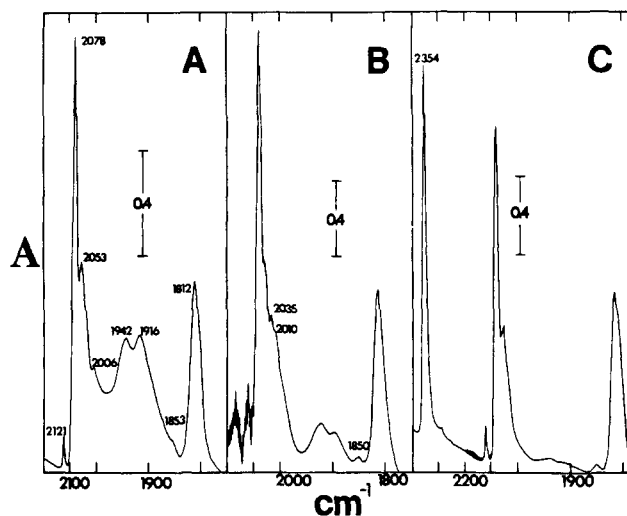


Figure 3. IR absorbance spectra: (A) $\text{Co}_2(\text{CO})_8$ sublimed onto Na-Y, in vacuo (total sublimation time 60 s, Na-Y pretreated at 675 K for 3 h); (B) results of 36-h exposure of sample in (A) to 450 torr of CO; (C) sample in (B) evacuated briefly and then exposed to 20 torr of O_2 .

$(\text{CO})_{12}$. It is noteworthy, though, that the bridging CO frequencies in Figure 2 are about 30 cm^{-1} lower and the terminal CO frequencies about 10–15 cm^{-1} higher than for both $\text{Co}_2(\text{CO})_8$ and $\text{Co}_4(\text{CO})_{12}$ on silica. Spectra in Figure 2B,D also contain three or four fairly broad features in the 1850–2000- cm^{-1} region that develop along with the several bands assigned to $\text{Co}_4(\text{CO})_{12}$.

The spectra shown in Figure 3 demonstrate that the broad bands in the 1850–2000- cm^{-1} region and the set of bands (2121, 2078, 2053, 1851, 1812 cm^{-1}) assigned to $\text{Co}_4(\text{CO})_{12}$ are due to different species. Exposure to CO results in the

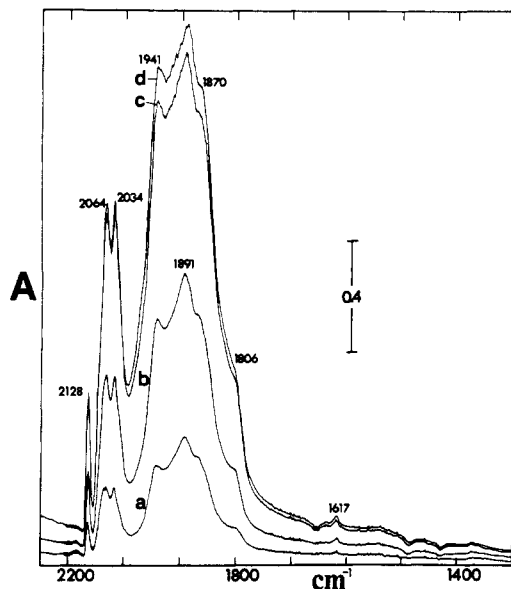


Figure 4. Difference IR absorbance spectra in the region 1300–2300 cm^{-1} of $\text{Co}_2(\text{CO})_8$ sublimed onto Na-X zeolite that had been pretreated at 675 K, in vacuo, for 4 h. Cell contained 23 torr of CO. Exposure time to $\text{Co}_2(\text{CO})_8$ (min): (a) 15; (b) 33; (c) 68; (d) 83, with the source of $\text{Co}_2(\text{CO})_8$ closed at 68 min.

gradual reduction of the intensity of bands between 1850 and 2000 cm^{-1} and the development of features near 2100 and 2035 cm^{-1} , but there is very little change in the $\text{Co}_4(\text{CO})_{12}$ bands. A more dramatic effect is obtained by exposure of the sample to just 20 torr of O_2 . The 1850–2000- cm^{-1} bands disappear rapidly, while the $\text{Co}_4(\text{CO})_{12}$ bands only diminish slightly in intensity; a new intense feature at 2354 cm^{-1} , due to adsorbed CO_2 , is observed for the first time, and some CO is released, as shown by the weak PQR structure near 2140 cm^{-1} , which is due to $\text{CO}(\text{g})$.

$\text{Co}_4(\text{CO})_{12}$ was sublimed directly onto a Na-Y zeolite to test the assignment of bands in spectrum 2Dm to $\text{Co}_4(\text{CO})_{12}$. The spectrum obtained immediately after overnight exposure to $\text{Co}_4(\text{CO})_{12}$ vapor but prior to evacuation of the cell displayed the bands assigned to $\text{Co}_4(\text{CO})_{12}$ in spectrum 2Dm and a set of weak bands at 2109, 2058, and 1862 cm^{-1} , typical of crystalline $\text{Co}_4(\text{CO})_{12}$. These three bands disappear from the spectrum upon evacuation. The remaining spectrum of $\text{Co}_4(\text{CO})_{12}/\text{Na-Y}$ is much weaker, though, than that of $\text{Co}_4(\text{CO})_{12}$ obtained by sublimation of $\text{Co}_2(\text{CO})_8$. Even extended exposure of the zeolite to $\text{Co}_4(\text{CO})_{12}$ vapor does not intensify this spectrum. These observations are consistent with weak physisorption of some $\text{Co}_4(\text{CO})_{12}$, which can be easily removed in vacuo, while other $\text{Co}_4(\text{CO})_{12}$ molecules adsorb more strongly at specific sites on the exterior zeolite surfaces and are not desorbed at room temperature. The carbonyl frequencies of these strongly adsorbed molecules are shifted from those for $\text{Co}_4(\text{CO})_{12}$ in solution, but the intensity pattern is not significantly affected.

In a separate experiment, $\text{Co}_2(\text{CO})_8$ was introduced onto Na-Y zeolite via solution impregnation. The spectrum obtained is very similar to that obtained by sublimation onto the support except that the new lower frequency bands between 1850 and 2000 cm^{-1} are more intense than in spectra of samples prepared by sublimation of $\text{Co}_2(\text{CO})_8$ onto the zeolite.

On Na-X Zeolites. A similar set of products, but with significant differences in distribution, is obtained upon sublimation of $\text{Co}_2(\text{CO})_8$ onto Na-X zeolite. When a Na-X wafer, pretreated by vacuum heating at 675 K, is exposed to $\text{Co}_2(\text{CO})_8$ vapor at room temperature, the observed color changes from white through yellow to dark olive green as the loading progresses, and CO is evolved as a result of the initial

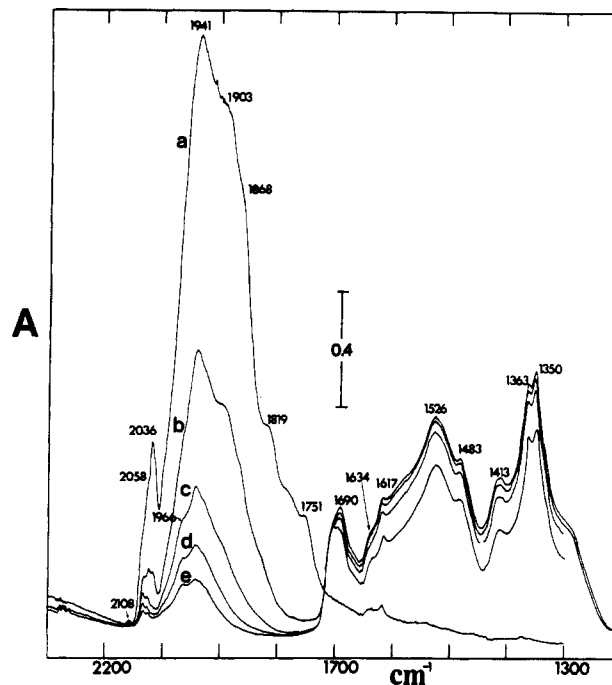


Figure 5. Continuation of series of spectra in Figure 4. Sample after evacuation of CO from cell to 10^{-2} torr for 33 min is given in (a). Spectra b–e show results for increasingly larger doses of $^{18}\text{O}^{18}\text{O}$. Total pressure in the cell (torr) at the time spectra were recorded and the time (min) that elapsed between each O_2 dosing and recording of the spectra are as follows: (b) 2, 2; (c) 3, 2; (d) 7, 4; (e) 17, 4. Pressures are due to the partial pressure of any unreacted O_2 and the pressure of gaseous products of the reaction—primarily CO_2 and CO.

$\text{Co}_2(\text{CO})_8/\text{Na-X}$ interaction. Figure 4 displays spectra obtained during the sequence of loading the dicobalt species by sublimation, under CO, onto the Na-X support. Bands at 2128, 2064, 2034, and 1806 cm^{-1} , due to $\text{Co}_2(\text{CO})_8$, appear. The most marked difference between the spectra on Na-X and Na-Y supports is the immediate development of the intense set of bands at 1941, 1891, and 1871 cm^{-1} on Na-X. Bands do not appear in this region for the $\text{Co}_2(\text{CO})_8$ on Na-Y zeolite until the CO has been removed and conversion to $\text{Co}_4(\text{CO})_{12}$ effected (Figure 2). Removal of CO from the cell induces changes in the high-frequency $\nu(\text{CO})$ bands indicative of conversion of $\text{Co}_2(\text{CO})_8$ to $\text{Co}_4(\text{CO})_{12}$ (Figure 5a). Comparison of Figure 5a and Figure 4d shows a significant intensity decrease of the 2030–2110- cm^{-1} bands relative to the 1941- cm^{-1} band when CO is removed from the sample cell.

Manometric Measurements. As is mentioned above, the IR spectrum obtained when $\text{Co}_2(\text{CO})_8$ is sublimed onto Na-X zeolite is dominated by the intense bands at 1871, 1891, and 1941 cm^{-1} ; only very weak bands due to the parent carbonyl are present. This suggests nearly complete conversion to the new product(s). To obtain stoichiometric information about the new product(s), manometric measurements were conducted in which a cobalt carbonyl/Na-X zeolite sample, with an IR spectrum like that in Figure 5a, was decomposed and oxidized at elevated temperature to liberate all carbon as CO or CO_2 . The measured volume of evolved gas and the analysis for cobalt in the sample provided a measure of the ratio of carbonyl to cobalt atoms for the species producing spectrum 5a. To provide the quantities of gas needed for accurate manometric measurement, the cell described in ref 2 was used with both the IR pellet cradle and bucket assembly to hold large quantities of pellet shards.

Sublimation of $\text{Co}_2(\text{CO})_8$, in vacuo, was followed by the sequential decomposition and oxidation steps described in Table II. The sum of the LN_2 condensable and noncondensable carbon-containing gases evolved as the sample was

Table II. Manometric Data for a Sample^a of Co₂(CO)₈ on Na-X

item	CCNTP	mol × 10 ⁴	C/Co
1. CO evolved from the sample as it was heated to 675 K ^{b,c}	2.43	1.09	1.94
2. LN ₂ condensables evolved from the sample as it was heated to 675 K	0.13	0.06	0.11
3. CO ₂ evolved from the sample after heating in closed cell under O ₂ at 675 K ^d	0.62	0.27	0.48
		total	2.5 ± 0.3

^a Sample mass is 128 mg with 2.6 ± 0.2% cobalt. Total cobalt content is (5.6 ± 0.5) × 10⁻⁵ mol. ^b Manometric measurements are subject to a random error range of ±0.02 mol × 10⁻⁴.

^c Significant pressure burst observed at 425 K. ^dNo LN₂ noncondensables were present. Oxidation of residual carbon to CO₂ was considered complete.

heated to 675 K, then oxidized at that temperature by O₂, amounted to 2.5 ± 0.3 mol/mol of cobalt in the sample.

Reaction with Oxygen and with ¹³CO. Figure 5 exhibits the spectra obtained when CO is removed from the Co₂(CO)₈/Na-X sample (spectrum 5a) and the sample is exposed to small doses of ¹⁸O¹⁸O. The individual doses provided insufficient oxygen to oxidize all the cobalt carbonyl species in the sample. As may be seen, the bands at 2036, 1941, 1903, and 1868 cm⁻¹ disappear allometrically as the several oxygen doses are added, and only a few very weak features, due to Co₄(C-O)₁₂, remain at the end of the entire sequence. A new set of bands between 1690 and 1350 cm⁻¹ develops as the ν(CO) bands disappear.

As is the case for silica- and alumina-supported cobalt carbonyls, oxidation by O₂ releases CO as well as CO₂. When the oxygen is ¹⁸O¹⁸O, the CO released upon oxidation of the cobalt carbonyl/zeolite includes as much as 50% C¹⁸O. A similar observation of C¹⁸O was reported in another paper¹ when silica-supported cobalt carbonyls were oxidized.

Facile exchange of ¹³CO for ¹²CO has been reported for other metal carbonyls on oxide supports.^{1,3,4} The exchange also takes place quite readily for Co₄(CO)₁₂ on X and Y zeolites. Figure 6 displays the series of spectra recorded over a period of 3 h when an excess of ¹³CO is added to a sample with the spectrum of Co₄(CO)₁₂ on Na-Y zeolite. This sample first had been exposed to O₂ to oxidize those species responsible for the 1850–2000-cm⁻¹ bands. (The weak low-frequency band near 1740 cm⁻¹ in Figure 6G is not due to Co₄(CO)₁₂ but is a new band, due to an unidentified species, which develops, in all cases, during exposure of the sample to CO. This band is at 1775 cm⁻¹ for ¹²CO.)

Studies on H-Y Zeolite. The ν(OH) region of sodium zeolites provides little information regarding the nature of the interactions between the cobalt carbonyls and the zeolite framework, but H⁺-exchanged zeolites, prepared by cation exchange of NH₄⁺ for Na⁺, have OH stretching frequencies that can be studied to obtain information about the interaction of the adsorbate with the zeolite. Figure 7 shows the sequence of spectra obtained as a deuterium-exchanged H-Y zeolite is loaded by sublimation of Co₂(CO)₈ under CO (Figure 7a–e) and as the transformation to Co₄(CO)₁₂/zeolite is achieved by removal of the CO (Figure 7f). As may be seen, the ν(OD) spectral region is perturbed by the addition of Co₂(CO)₈. The sharp band at 2690 cm⁻¹ in the D-Y spectrum, which is due to OD stretches at O-1 and O-2 sites within the zeolite supercages,⁶ corresponds to a sharp feature at 3645 cm⁻¹ in H-Y

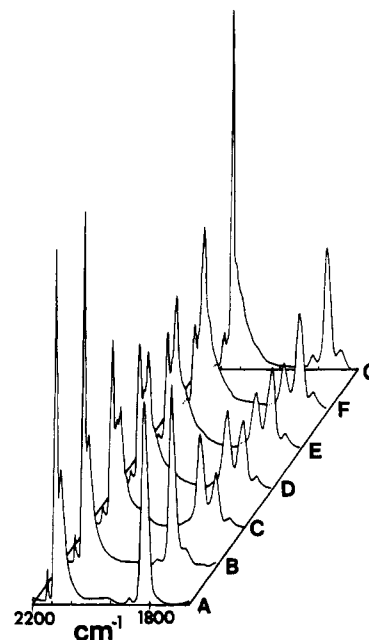


Figure 6. Difference IR absorbance spectra in the ν(CO) region showing the results for ¹³CO/¹²CO isotopic exchange on Co₄(CO)₁₂/Na-Y. The spectra were recorded after the following cumulative exposure times (min) to a gas phase initially containing 26 torr of ¹³CO, providing a total ¹³CO/¹²CO ratio for the sample of about 20/1: (A) 0; (B) 3; (C) 40; (D) 70; (E) 110; (F) 180; (G) recorded after evacuation followed by overnight exposure to a fresh dose of 15 torr of ¹³CO.

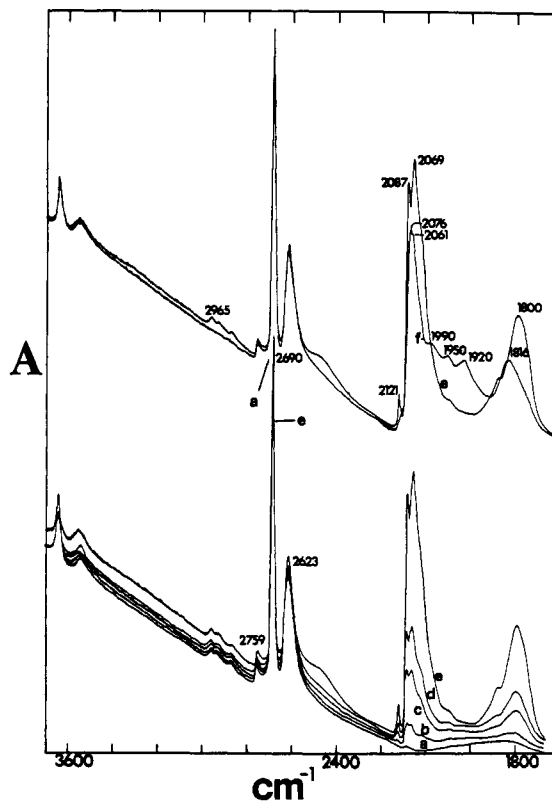


Figure 7. IR absorbance spectra in the region 1700–3700 cm⁻¹ for Co₂(CO)₈ sublimed onto D-Y zeolite prepared by exposure of H-Y zeolite to 56 torr of D₂ for 1 h at 675 K. Exposure times for D-Y to Co₂(CO)₈ vapor under 16 torr of CO (min): (a) 6; (b) 41; (c) 86; (d) 106; (e) 123. Spectrum f shows the result of reducing CO pressure to 10⁻² torr after closing the tube containing Co₂(CO)₈.

(6) (a) Rees, L. V. C.; Williams, C. J. *Trans. Faraday Soc.* **1965**, *61*, 1481. (b) Olson, D. H.; Dempsey, E. J. *Catal.* **1969**, *13*, 221. (c) Ward, J. H. "Molecular Sieve Zeolite. I"; Gould, R. F., Ed.; American Chemical Society: Washington, DC, 1971; Adv. Chem. Ser. No. 101, pp 380–404.

zeolite. Upon addition of Co₂(CO)₈, the 2690 O-D stretch is reduced in intensity and a broad band centered near 2470

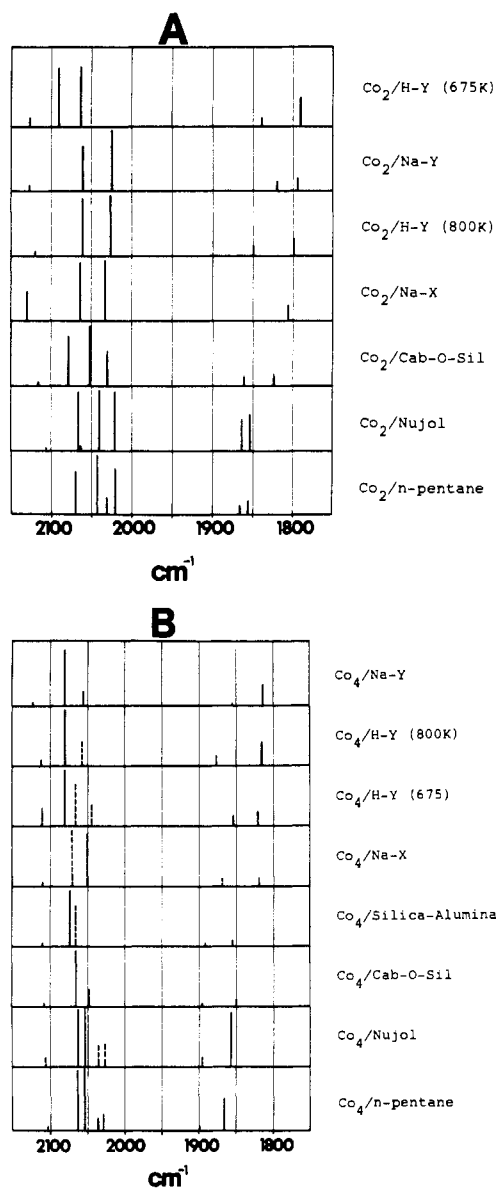


Figure 8. Comparison of $\nu(\text{CO})$ frequencies in various environments for (A) $\text{Co}_2(\text{CO})_8$ and (B) $\text{Co}_4(\text{CO})_{12}$. The relative intensities implied by the bars are based on normalization to the most intense band for each compound. The broken bars represent bands appearing as poorly defined shoulders nearly obscured by intense bands of $\text{Co}_4(\text{CO})_{12}$, itself, or another species present. The relative intensity and frequency positions of other bands are, therefore, less precise than for the bands represented by solid bars.

cm^{-1} develops. Conversion to $\text{Co}_4(\text{CO})_{12}$ reduces the intensity of this 2470 cm^{-1} band but does not entirely remove it from the spectrum. The same study conducted with an H-Y zeolite resulted in a shift of the 3645-cm^{-1} $\nu(\text{OH})$ band to about 3350 cm^{-1} .

Discussion and Conclusions

Nature of Binding to Surfaces. The IR experiments for $\text{Co}_2(\text{CO})_8$ sublimed onto H-Y and D-Y zeolites indicate the cobalt carbonyl binds to the H^+ -exchanged zeolite via H bonding. The magnitude of $\Delta\nu(\text{OH})$ for the hydroxyl groups affected is comparable to shifts observed upon adsorption of acetonitrile and acetone on hydroxylated oxide surfaces. Heats of adsorption in the range 4–6 kcal/mol have been measured for such adsorbents on silica gels when $\Delta\nu(\text{OH})$ is $300\text{--}400 \text{ cm}^{-1}$.⁷

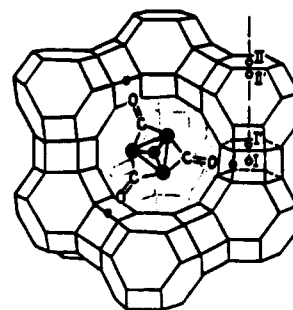
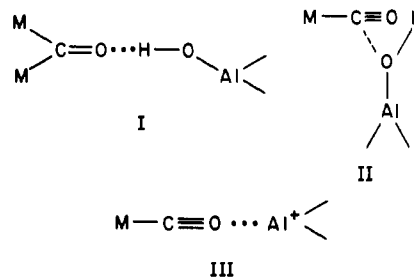


Figure 9. Scale diagram of faujasite supercages looking through aperture from one cage into another. Dots locate O-1 oxygens. Diagram shows two-dimensional projection of $\text{Co}_4(\text{CO})_{12}$ over window. Terminal CO ligands are deleted.

The shifts in $\nu(\text{CO})$ frequencies for both $\text{Co}_2(\text{CO})_8$ and $\text{Co}_4(\text{CO})_{12}$ are consistent with H bonding to the bridging carbonyls. Figure 8 compares the $\nu(\text{CO})$ values for $\text{Co}_2(\text{CO})_8$ and $\text{Co}_4(\text{CO})_{12}$ in various environments, including oxide support surfaces. The expected direct effect of hydrogen bonding to the basic oxygens of the bridging carbonyls is the observed shift ($40\text{--}60 \text{ cm}^{-1}$) to lower frequency for these oscillators. The upward shift of the terminal $\nu(\text{CO})$ values ($10\text{--}20 \text{ cm}^{-1}$) is the indirect effect of the movement of electrons away from the metal atom and toward the bridging CO's upon H-bond formation, leaving less electron density for $\text{M}(\text{d}\pi) \rightarrow \text{CO}(\pi^*)$ back-bonding to the terminal carbonyls. Besides increasing the stretching frequencies of these groups, the decreased electron density at the carbonyl carbon makes them more susceptible to nucleophilic attack, as will be discussed below.

Three modes of interaction of metal carbonyls with an alumina surface have been described by Brown⁸ and are shown.



Mode III would exist on a fully dehydroxylated alumina surface on which Lewis acid sites have formed; it is, therefore, not expected for the zeolite samples discussed here. The bonding in mode I best explains the $\nu(\text{CO})$ and $\nu(\text{OH})$ shifts on H-Y zeolite and silicas. But, it is conceivable that interaction via mode II, at terminal CO's, also could occur in these samples; indeed, H bonding to bridging CO's (mode I) should increase the propensity toward mode II interaction with terminal ligands in the same molecule. There is no IR evidence for stable interactions of the mode II type in these samples, but an intermediate of this type could be a prelude to some of the chemistry observed for cobalt carbonyls on aluminas and zeolites.

The pattern of intensities for the $\nu(\text{CO})$ bands of $\text{Co}_2(\text{CO})_8$ and $\text{Co}_4(\text{CO})_{12}$ within the zeolite remains essentially that observed for solution spectra of these species, despite shifts due to H bonding. This and the absence of new bands or shoulders associated with these adsorbed species indicate the symmetry of the compounds is not significantly perturbed by adsorption. A likely adsorption site within the zeolite, which would provide a C_{3v} symmetry environment, is illustrated in

(7) Kiselev, A. V. *Surf. Sci.* **1965**, *3*, 292.

(8) Brown, T. L. *J. Mol. Catal.* **1981**, *12*, 41.

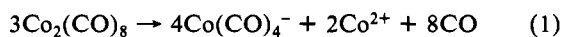
the scale diagram in Figure 9. The C_{3v} symmetry about the supercage windows and the close match of distances between alternate O-1 hydroxyls at site III (6.8 Å) with the distances between oxygens of bridging carbonyls of $Co_4(CO)_{12}$ (6.7 Å) suggest this as a likely site of H bonding for this molecule in the H-Y zeolite. Ballivet-Tkatchenko and Coudurier have reported a study of $Fe_3(CO)_{12}$ on H-Y zeolite in which $\Delta\nu(OH)$ and $\Delta\nu(CO)$ show similitude with those shifts observed for the cobalt carbonyls on the zeolite. Those investigators also propose H bonding near the supercage windows.⁹

Although Na-Y and Na-X zeolite do not have hydroxyl protons for H bonding or properly located sodium ions for a Lewis interaction at the appropriate positions about the supercage windows, an electrostatic interaction in the supercage may result in similar binding geometry. The $\nu(CO)$ shifts for the cobalt carbonyls on the sodium zeolite supports could be due primarily to electrostatic interactions as suggested by theoretical calculations that predict the electrostatic fields in the vicinity of site III for a zeolite should cause substantial changes in the energies of bonding electrons in adsorbed molecules.¹⁰

The separation between oxygens of the bridging carbonyls in $Co_2(CO)_8$ is nearly the same as for $Co_4(CO)_{12}$. Hydrogen bonding of this molecule to two alternate O-1 hydroxyls at the supercage window would leave one O-1 site available for a second molecule of $Co_2(CO)_8$. (The O-1 sites not marked in the diagram of Figure 9 are blocked by the terminal CO ligands and are, therefore, not accessible to the bridging ligands.) Bonding of this second molecule at this site through one bridging CO would put the two molecules in proper juxtaposition for reaction to form $Co_4(CO)_{12}$.

The very low loading levels achieved when $Co_4(CO)_{12}$ is sublimed directly onto X and Y zeolites and the inability to extract $Co_4(CO)_{12}$ or any other cobalt carbonyl species from a zeolite sample, when the IR spectrum is dominated by bands due to $Co_4(CO)_{12}$, are evidence for the inability of this species to pass through the supercage apertures. This is expected on the basis of the calculated kinetic diameter of $Co_4(CO)_{12}$ (9.6 Å) and the faujasite window openings (8.0 Å) and is not the first example of formation, within the zeolite, of a metal cluster carbonyl that is too large to escape the zeolite cavities. Gelen et al. have proposed the development of $Rh_n(CO)_m$ ($n = 6-13$) by carbonylation of zerovalent rhodium in a Na-Y zeolite.¹¹

Stoichiometry of Surface Reactions. The cobalt carbonyl on Na-X zeolite (Figure 5a) contained 2.5 ± 0.3 mol of carbon/mol of Co present (Table II). The intense $\nu(CO)$ bands at 1941, 1891, and 1870 cm^{-1} on the Na-X are very similar to the set of bands observed when $(CO)_9Co_3CCH_3$ reacts with alumina and zeolite and that were assigned to $Co(CO)_4^-$ in that study.² The presence of $Co(CO)_4^-$ as a major species implies disproportionation of the parent carbonyl. To achieve a ratio of about 2.5 CO/Co, with some Co existing as $Co(CO)_4^-$, requires substantial or total decarbonylation of the remaining cobalt. This might be the fate of the positively charged cobalt formed in the disproportionation. Indeed, disproportionation, as in reaction 1, would evolve CO and leave a product on the zeolite with 2.7 mol of CO/mol of cobalt, in good agreement with the measured value of 2.5 ± 0.3 .



The increased tendency toward disproportionation to $Co(CO)_4^-$ and cobalt ions when the support is Na-X, as compared with Na-Y zeolite, is consistent with the greater basicity

of the Na-X and with the larger electrostatic field that would stabilize ions within the supercages of this high alumina content zeolite.¹⁰

Mechanistic Aspects. Brown has presented models and mechanisms for the adsorption and reactions of metal carbonyl compounds on transition aluminas.⁸ Those discussions emphasize the interactions of the metal carbonyl with the alumina surface at *elevated temperatures*; mechanisms of reactions leading to decarbonylation, evolution of CO, CO_2 , CH_4 , and H_2 , and the oxidation of the transition-metal center were postulated. Most of the results reported in this and another paper¹ are for room-temperature reactions of the cobalt carbonyls on oxide supports. These reactions involve, first, the conversion of $Co_2(CO)_8$ to $Co_4(CO)_{12}$ with evolution of CO but also, on the more active surfaces, the partially reversible decarbonylation of the cobalt carbonyls to generate novel sub-carbonyls and $Co(CO)_4^-$. Irreversible decarbonylation occurs only at elevated temperatures, presumably because the cobalt is oxidized under those conditions.

The observed room-temperature reactions of the cobalt carbonyls on the oxide surfaces may be explained by considering them to be analogues of known solution reactions of these carbonyls. Dicobalt octacarbonyl is known to react with bases according to the general reaction first proposed by Wender et al.¹⁴ This reaction provides basic ligands to stabilize the cobalt cations formed in reaction 1. Reaction 2 is thought to

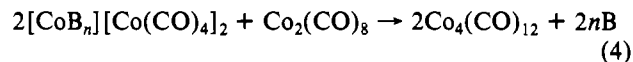


consist of several steps, including the initial development of an unstable base-complexed metal carbonyl cation $[BCo(CO)_4]^+$. Cationic metal carbonyl complexes have decreased electron density at the carbonyl carbon and are, therefore, more susceptible to attack by nucleophilic bases. A base-coordinated cobalt carbonyl cation may be quickly decomposed through attack by surface oxide or hydroxide groups of the zeolite or alumina surfaces.

Chini and co-workers^{15,16} found that the reaction of $Co_2(CO)_8$ with alcohols (as bases) could proceed beyond the initial disproportionation (2) to yield a polynuclear anion, $Co_6(CO)_{15}^{2-}$, according to reaction 3. The yields of $Co_6(CO)_{15}^{2-}$



were very sensitive to the alcohol (base) employed, with EtOH providing the best yield. When B = IPA or *t*-BuOH, though, only $Co_4(CO)_{12}$ and minor quantities of $Co(CO)_4^-$ were obtained. It is believed that the bulky nature of these two alcohols makes it impossible to form the stable six-coordinate complexes of Co(II) that are necessary for $Co_6(CO)_{15}^{2-}$ production. Chini suggested reaction 4 occurs when B is a sterically crowded base.



The basicity of the silanol groups on a silica surface has been compared with that of alcohols.¹⁷ The surface silanols might, therefore, function as bases that induce reaction 2 on the silica. Viz.:

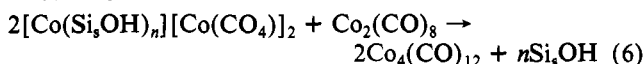


The silanols would not, however, be expected to provide the octahedral coordination necessary to stabilize the Co(II) but

(9) Ballivet-Tkatchenko, D.; Coudurier, G. *Inorg. Chem.* **1979**, *18*, 3.
 (10) Barhomeuf, D. *J. Phys. Chem.* **1979**, *83*, 249.
 (11) Gelen, P.; Ben Taarit, Y.; Naccache, C. *J. Catal.* **1979**, *59*, 357.
 (12) Bor, G. *Spectrochim. Acta* **1963**, *19*, 1209.
 (13) Haas, H.; Sheline, R. K. *J. Chem. Phys.* **1967**, *47*, 2996.

(14) Wender, I.; Steinberg, H. W.; Orchin, M. *J. Am. Chem. Soc.* **1952**, *74*, 1216.
 (15) Chini, P.; Albano, V. *J. Organomet. Chem.* **1968**, *15*, 433.
 (16) Chini, P. *Pure Appl. Chem.* **1970**, *23*, 489.
 (17) Iler, R. K. "The Chemistry of Silica"; Wiley-Interscience: New York, 1979.

would act like IPA or *t*-BuOH, promoting the formation of $\text{Co}_4(\text{CO})_{12}$ via reaction 6.



On X and Y zeolites, a species identified as $\text{Co}(\text{CO})_4^-$ is detected upon removal of CO from the sample. These aluminosilicates have basicities appropriate for the promotion of reactions 5 and 6, but sites within the zeolite supercage or sodalite cages could provide for multiple coordination of the cobalt cations. This and the electrostatic fields within the zeolite might stabilize the cations formed in (5) and prevent some of the cobalt from reacting via (6) to form $\text{Co}_4(\text{CO})_{12}$. These zeolite coordination sites may also stabilize sub-carbonyls responsible for the several bands between 1850 and 2030 cm^{-1} , which develop in the IR spectra during the conversion of $\text{Co}_2(\text{CO})_8$ to $\text{Co}_4(\text{CO})_{12}$ and $\text{Co}(\text{CO})_4^-$. $[\text{Co}_6(\text{CO})_{15}]^{2-}$ might also be formed via reaction 3, but the $\nu(\text{CO})$ bands observed bear very little resemblance to the spectra reported for this hexanuclear anion, nor does the $\nu(\text{CO})$ spectrum of any other known polynuclear cobalt carbonyl species correspond with the observed set of bands between 1930 and 2030 cm^{-1} , assigned here to one or more sub-carbonyls.

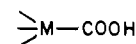
Heating the zeolite-supported $\text{Co}_4(\text{CO})_{12}$ to 350 K causes the reversible conversion of the $\text{Co}_4(\text{CO})_{12}$ to cobalt carbonyl species with broad bands near 2030 and 1950 cm^{-1} . This may be a $\text{Co}_4(\text{CO})_{12-n}$ compound stabilized through coordination by surface hydroxyls at the vacant sites developed by the thermal decarbonylation. Heating to 425 K and above leads, on silicas, alumina, and zeolites, to irreversible loss of the $\nu(\text{CO})$ spectrum, the evolution of CO_2 and CO, and the formation of surface carbonates, presumably via the decarbonylation and decarboxylation steps outlined by Brown⁸ to produce oxidized cobalt. Like oxidized cobalt formed from cobalt salts on the same oxide surfaces,¹⁸ the cobalt formed by heating these samples above 425 K is not easily reduced by H_2 and CO. Recently initiated studies of cobalt carbonyls on the strongly basic support, MgO, disclosed the formation of a stable species with bands at 2030, 1940, and 1870 cm^{-1} that may be reversibly decarbonylated by heating at temperatures as high as 675 K. The more strongly basic sites on MgO may coordinate the decarbonylated form and stabilize it against oxidation by the surface. Studies of this system are continuing.¹⁹

Oxidation Reactions and Formation of C^{18}O . As illustrated in Figure 5, reaction of the supported cobalt carbonyl species with $^{18}\text{O}^{18}\text{O}$ generates surface carbonates. Bands between 1690 and 1350 cm^{-1} in the IR spectra (Figure 5b-e) are due to zeolite carbonates containing oxygen-16 or oxygen-18.² At least one band in this region—at 1543 cm^{-1} when $^{16}\text{O}^{16}\text{O}$ is the oxidant and at 1526 cm^{-1} when $^{18}\text{O}^{18}\text{O}$ is used—does not appear in reports of IR spectra for carbonates on zeolites. This band may be due to a cobalt carbonate; this assignment is supported by the blue color of the oxidized samples.

As is the case for the cobalt carbonyls on the silica-alumina support,¹ C^{18}O is liberated upon oxidation by $^{18}\text{O}^{18}\text{O}$. Reactions of the cobalt carbonyls with oxygen generally evolved more CO than CO_2 in the product gases. The evolution of CO in quantities equal to or exceeding the CO_2 indicates the spontaneous liberation of this ligand following oxidation of the cobalt. The appearance of C^{18}O in this evolved CO when the oxidant is $^{18}\text{O}^{18}\text{O}$ suggests reversibility in at least one of the oxidation steps.

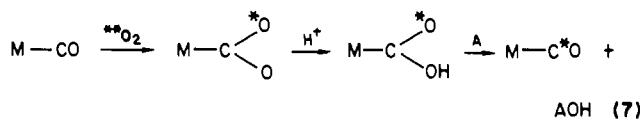
Muetterties has reported oxygen exchange from H_2^{18}O into the carbonyl ligands of $\text{Re}(\text{CO})_6^+$,²⁰ and Darensbourg et al.

have more recently reported the formation of highly oxygen-labeled $[\text{M}(\text{CO})_{6-n}\text{L}_n]^+$, $\text{M}(\text{CO})_{6-n}\text{L}_n$, and $\text{M}(\text{CO})_5$ species by reaction of $^{18}\text{OH}^-$ with metal carbonyls.²¹⁻²³ Incorporation of ^{18}O from water or OH^- ligands must occur via reversibly formed

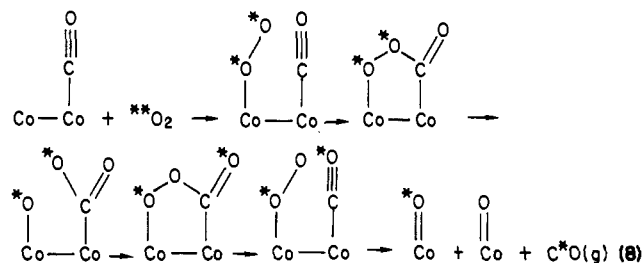


species. The rate and degree of oxygen exchange is greatest for the most electrophilic carbonyl carbons; viz., cationic metal carbonyls exchange most rapidly, while metal carbonyls highly substituted by electron-donating ligands exchange only slowly, if at all.

The large fraction of CO evolved in this study as C^{18}O (as much as 50% of the total in some cases) suggests the oxygen is not incorporated by an indirect route involving oxidation of some CO to labeled CO_2 in the gas phase, exchange of this CO_2 with oxygen of surface hydroxyls, and reversible reaction of these labeled hydroxyls with the CO ligands. This process necessarily would produce far lower percentages of ^{18}O incorporation into the CO than are observed. Rather, a scheme like that in (7) may be operant. In this scheme H^+ and A (acid site) are surface species; A may be a second proton. Zerchina²⁴ has reported evidence for $(\text{CO})_n\text{MCO}_2$ ($\text{M} = \text{Mo}, \text{Cr}, \text{W}, \text{Ni}, \text{Fe}$) for metal carbonyls on MgO.

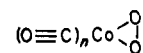


An alternative route to C^{18}O would involve a peroxyformate intermediate as in reaction 8. The dioxygen complex, $\text{Co}(\text{CO})_4\text{O}_2$,



has been detected by EPR at 77 K upon reaction of $\text{Co}_2(\text{CO})_8$ with O_2 . The small hyperfine coupling interaction with ^{59}Co in this species indicates the unpaired electron is largely confined to the dioxygen group, meaning the formulation $[\text{Co}(\text{CO})_4]^+\text{O}_2^-$ is reasonable.²⁵ The nucleophilic superoxide anion and relatively electrophilic carbonyl carbons in the cationic complex could be expected to react as shown in the second step of (8).

Other dioxygen cobalt carbonyl species of the form



have been reported from studies of the cocondensation of Co, CO, and O_2 in matrices at 10–12 K,^{26,27} and structures similar

- (20) Muetterties, E. L. *Inorg. Chem.* **1965**, *4*, 1841.
 (21) Darensbourg, D. J.; Darensbourg, M. Y. *Inorg. Chem.* **1978**, *17*, 3300.
 (22) Darensbourg, D. J.; Darensbourg, M. Y.; Walker, N.; Froelich, J. A.; Baous, H. L. C. *Inorg. Chem.* **1979**, *18*, 1401.
 (23) Darensbourg, D. J.; Baldwin, B. J.; Froelich, J. A. *J. Am. Chem. Soc.* **1980**, *102*, 4688.
 (24) Guglielminotta, E.; Zerchina, A. *J. Chim. Phys.* **1981**, *78*, 891.
 (25) Fieldhouse, S. A.; Fullman, B. W.; Neilson, G. W.; Symons, M. C. R. *J. Chem. Soc., Dalton Trans* **1974**, 567.
 (26) Hanlan, L. A.; Huber, H.; Kundig, E. P.; McGarvey, B. R.; Ozin, G. A. *J. Am. Chem. Soc.* **1975**, *97*, 7054.
 (27) Ozin, G. A.; Hanlan, A. J. L.; Power, W. J. *Inorg. Chem.* **1979**, *18*, 2390.

(18) Anderson, R. B.; Dawson, P. T., Eds. "Experimental Methods in Catalytic Research"; Academic Press: New York, 1976; Vol. II.
 (19) Gopal, P.; Watters, K. L. *Proc. Int. Congr. Catal.* **1984**, *8*.

to those in reaction 8 have been proposed in the photolytic oxidation of $\text{Cr}(\text{CO})_6$ cocondensed with O_2 in argon matrices, although no evolved C^{18}O was detected in that study when the oxygen was $^{18}\text{O}^{18}\text{O}$.²⁸ The evolution of CO with as much as

50% C^{18}O in this study requires, of course, that each step in (8) be reversible.

No experimental information is available that would permit a distinction between reactions 7 and 8 as the route to C^{18}O .

Acknowledgment. This research was supported by grant No. CHE 77-20373 from the National Science Foundation.

Registry No. $\text{Co}_2(\text{CO})_8$, 10210-68-1; $\text{Co}_4(\text{CO})_{12}$, 17786-31-1.

(28) Poliakoff, M.; Smith, K. P.; Turner, J. J.; Wilkinson, A. J. *J. Chem. Soc., Dalton Trans.* 1982, 651.

Contribution from the Department of Chemistry,
University of Virginia, Charlottesville, Virginia 22901

Empirical Intensity Parameters for the $4f \rightarrow 4f$ Absorption Spectra of Nine-Coordinate Neodymium(III) and Holmium(III) Complexes in Aqueous Solution

EILEEN M. STEPHENS, SCOTT DAVIS,[†] MICHAEL F. REID, and F. S. RICHARDSON*

Received February 7, 1984

Absorption spectra are reported for five different 1:3 Ho^{3+} :ligand systems in aqueous solution under alkaline pH conditions, and these spectra are compared to that obtained for the HoCl_3 salt in aqueous solution (pH \sim 2). The transition intensities observed in these spectra are analyzed in terms of the Judd-Ofelt parameterization scheme for lanthanide $4f \rightarrow 4f$ multiplet-to-multiplet transitions. A similar intensity analysis is reported for absorption results obtained previously on an analogous series of Nd(III) complexes. The values of the intensity parameters Ω_λ ($\lambda = 2, 4, 6$) determined for the various systems are compared, and variations in these values are discussed in terms of ligand structural properties.

Introduction

In two previous studies^{1,2} we have reported absorption spectra and $4f \rightarrow 4f$ oscillator strengths for a series of erbium(III)¹ and neodymium(III)² complexes in aqueous solution. The ligands included in those studies were oxydiacetate (ODA), dipicolinate (DPA), iminodiacetate (IDA), (methylimino)diacetate (MIDA), malate (MAL), and *N,N'*-ethylenebis(2-(*o*-hydroxyphenyl)glycinate) (EHPG),³ each of which has at least two donor moieties suitable for binding to a trivalent lanthanide ion in aqueous solution. The principal objectives were to examine the hypersensitivity of certain $4f \rightarrow 4f$ transition intensities to ligand binding, to correlate the observed hypersensitive behavior to ligand structural properties, and to relate the pH dependence of the hypersensitive transition intensities to complex formation. Intensity calculations were also reported for a set of model systems whose structures were chosen to mimic those of the $\text{Ln}^{3+}(\text{aq})$, $\text{Ln}(\text{ODA})_3^{3-}$, $\text{Ln}(\text{DPA})_3^{3-}$, $\text{Ln}(\text{IDA})_3^{3-}$, and $\text{Ln}(\text{MIDA})_3^{3-}$ complexes in solution.^{1,2} These calculations were based on a $4f \rightarrow 4f$ intensity model that includes both *static* point-charge crystal field effects and *dynamic* ligand-polarization effects.⁴⁻⁷

In our previous studies we reported oscillator strengths (calculated and empirically determined) for just a few of the observed $4f \rightarrow 4f$ transitions in the Er(III)¹ and Nd(III)² complexes, with special emphasis on the "hypersensitive" transitions. No attempts were made to extract general intensity parameters from the data. In the present study we report absorption results for a series of Ho(III) complexes that are analogous to the Er(III) and Nd(III) complexes examined previously. The oscillator strengths obtained from the absorption intensity data are used to determine Judd-Ofelt intensity parameters Ω_λ ($\lambda = 2, 4, 6$)⁸ for each system, employing standard "fitting" procedures. Using the results obtained in our previous study of Nd(III) complexes, we also carried out a parameterization of the Nd(III) intensity data within the

general Judd-Ofelt Ω_λ parameter scheme for multiplet-multiplet transitions.

The Ω_λ parameterization of $4f \rightarrow 4f$ (multiplet-to-multiplet) transition intensities has enormous utility for systematizing lanthanide intensity data. Excluding effects due to crystal field induced J-level mixings, the Ω_λ parameters in this scheme include *all* of the ligand-dependent effects contributing to $4f \rightarrow 4f$ electric dipole intensity. For a given lanthanide ion, differences in the Ω_λ parameters determined for different complexes can be attributed to differential ligand field effects associated with, for example, coordination numbers, coordination geometries, and the respective lanthanide-ligand pairwise interaction mechanisms. Expressed in terms of the Ω_λ parameters, the oscillator strength of an A \rightarrow B multiplet-to-multiplet transition is given by

$$f_{AB} = (8\pi^2 m_e c / 3h) \chi \bar{\nu}_{AB} g_A^{-1} \sum_{\lambda} \Omega_{\lambda} \left| \sum_{\psi J} \sum_{\psi' J'} C_A^*(\psi J) \times C_B(\psi' J') \langle \psi^N \psi | [S^L] J || U^{\lambda} || \psi'^N \psi' | [S^L] J' \rangle \right|^2 \quad (1)$$

where $\lambda = 2, 4$, and 6 , χ is the Lorentz field correction for the refractivity of the medium, $\bar{\nu}_{AB}$ is the A \rightarrow B transition energy (expressed in wavenumbers), g_A is the degeneracy of state A, U^{λ} is an intraconfigurational unit tensor operator, and the coefficients $C_A(\psi J)$ and $C_B(\psi' J')$ give the compositions of states A and B in terms of the "free-ion" f^N intermediate-coupling wave functions. In eq 1, the radial-dependent parts of the A and B state functions have been absorbed into the Ω_λ parameters, so these parameters do contain properties in-

- (1) Davis, S. A.; Richardson, F. S. *Inorg. Chem.* 1984, 23, 184.
- (2) Stephens, E. M.; Schoene, K.; Richardson, F. S. *Inorg. Chem.* 1984, 23, 1641.
- (3) The alternative name for EHPG is *N,N'*-bis(2-hydroxyphenyl)-ethylenedinitrilo-*N,N'*-diacetate.
- (4) Richardson, F. S.; Saxe, J. D.; Davis, S. A.; Faulkner, T. R. *Mol. Phys.* 1981, 42, 1401.
- (5) Richardson, F. S. *Chem. Phys. Lett.* 1982, 86, 47.
- (6) Morley, J. P.; Saxe, J. D.; Richardson, F. S. *Mol. Phys.* 1982, 47, 379.
- (7) Kirby, A. F.; Richardson, F. S. *J. Phys. Chem.* 1983, 87, 2544, 2557.
- (8) Peacock, R. D. *Struct. Bonding (Berlin)* 1975, 22, 83.

[†] Present address: Department of Chemistry, Dickinson College, Carlisle, PA.